Investigative Ophthalmology & Visual Science, Vol. 31, No. 3, March 1990

Microperfusion Studies on the Permeability of Retinal Vessels

A New Model Demonstrating Organic Anion Transport and a Reabsorptive Fluid Flux

J. N. Murta,* J. G. Cunha-Vaz,* C. A. Sabo,† C. W. Jones,† and M. E. Laski‡

We developed an experimental model to study the permeability of individual retinal vessels in vitro using microperfusion techniques adapted from kidney tubule studies. The retinal vessels were isolated by freehand dissection and mounted on a microperfusion apparatus. When inulin was perfused luminally, it was diluted to 80.2 ± 2.3% of its initial concentration. However, no radioactive leak into the bath side was observed, suggesting that the dilution was due to fluid flux from bath to lumen. The dilution of fluorescein (81.9 ± 3.8%) was in the same range as that of inulin, the reference marker. The extremely low lumen-to-bath fluorescein flux, $0.5 \pm 0.9 \times 10^{-12}$ mol/min/mm, increased by 68% when probenecid was added to the perfusate and by 210% when probenecid was placed in the bath. The effect was concentration-dependent. When placed in the bath, fluorescein moved rapidly across the retinal vessel walls, accumulating in the lumen to concentrations 40 times higher than in the bath. This movement from bath to lumen, which was much higher ($13.6 \pm 0.3 \times 10^{-12}$ mol/min/mm) than the lumen-to-bath fluorescein flux for the same fluorescein concentration, decreased by adding probenecid to the bath. The kinetics of this unidirectional movement of fluorescein were consistent with a saturable active transport process. The fluid flux from bath to lumen across the retinal vessels, which was 6.3 ± 1.0 nl/min/mm for perfusion rates of 6.6 ± 0.2 nl/min, was temperature-dependent and was coupled to the fluorescein transport. Fluorescein stimulated the fluid flux by 17% when added to the perfusate and by 60% when added to the bath, and this effect could be reversed by probenecid. Our results showed an active transport of fluorescein in the rabbit retinal vessels coupled with net fluid flux from outside the vessels into the lumen. Invest Ophthalmol Vis Sci 31:471–480, 1990

The alteration of the functional characteristics of the blood–retinal barriers appears to play a major role in the pathophysiology of retinal disease. The widespread use of fluorescein angiography and, more recently, the development of vitreous fluorophotometry have shown that a disturbance of these barriers may precede the retinal changes in diabetes and other retinal diseases.[1-3]

From the *Department of Ophthalmology, University of Coimbra, Coimbra, Portugal; the †Department of Ophthalmology, University of Illinois College of Medicine at Chicago, and the ‡Department of Medicine, Texas Tech University, Lubbock, Texas.

Supported by NIH Grant EY-06198 and CORE Grant EY-1792-07 from the NEI, Bethseda, Maryland; by a Lions Club International Feasibility Grant (American Diabetes Association); and by the Junta Nacional de Investigação Científica, Portugal (JNM).

Submitted for publication: October 13, 1988; accepted August 7, 1989.

Reprint requests: José G. Cunha-Vaz, Centro de Oftalmologia da Universidade de Coimbra, Hospitais da Universidade de Coimbra, 3000 Coimbra, Portugal.

The active transport of fluorescein, an organic anion, across the retina was described initially by Cunha-Vaz and Maurice,[4] but its site (presumably retinal vessels and retinal pigment epithelium) and mode of action remained uncertain. Recently, this transport mechanism has been confirmed,[5] and direct evidence of its location in the retinal pigment epithelium has been presented.[6] Studies on the retinal vessels, however, still are lacking.

We developed a new experimental model to investigate the permeability of the retinal vessels using microperfusion techniques adapted from kidney tubule studies.[7-9] Application of this technology to vascular physiology has been limited because of anatomic problems involved in isolating individual small vessels for microperfusion. Retinal vessels of rabbits are appropriate for these studies, because the rabbit vascular walls are free from surrounding glia and contact the vitreous fluid directly.[10] Ultrastructural and permeability studies have shown clearly that these vessels behave like true retinal vessels and have the fea-

tures that characterize blood–retinal barrier vessels in other species.[10,11]

Materials and Methods

These studies were performed using microperfusion techniques adapted from kidney tubule studies first described by Burg and co-workers.[7]

Dissection Technique

The investigations described adhered to the ARVO Resolution on the Use of Animals in Research. Male New Zealand white rabbits, weighing less than 2.5 kg each (1.8–2.2 kg), were decapitated. The eyes were removed quickly and placed in a Petri dish (diameter, 90 mm) containing cold (4°C) oxygenated, physiologic salt solution supplemented with 4% normal rabbit serum. Under a binocular dissecting microscope (Olympus stereo microscope, model SZ III; Woodbury, NY) the eyes were bisected at the ora serrata, and the anterior segment with adherent vitreous was separated from the posterior pole. A fiberoptic light source (Dolan-Jenner Illuminator, 180 dual branch fiberoptic; Scientific Supply, Chicago, IL) illuminated the tissue. The Petri dish was placed on black paper so that the vessels, in contrast to the black, could be seen clearly.

The visible vessels were confined to wing-shaped areas of medullated nerve fibers that were extended horizontally on either side of the disc, and lay in the vitreous free from surrounding glia.[4,10] Individual retinal vessels, apparently arterioles, were stripped away with jeweller forceps by freehand dissection, and a relatively long, unbranched segment of vessel was isolated after its ends were cut with sharp scissors. It was necessary to make the final cuts with the finest possible instruments at temperatures no higher than 4°C. Without these precautions, a spasm of the vessel and closure of the lumen could have occurred, making cannulation difficult or impossible and possibly resulting in structural damage. The perfused length of rabbit retinal vessels varied between 0.18 and 0.48 mm.

Transfer of the Vessels

To avoid pulling the vessels through an air–water interface, we transported them to the perfusion chamber with a transfer pipette (made from a Pasteur pipette, bent at a 45° angle). The tip was fire-polished to prevent adherence of vessels. A metal holder supported the pipette, while a screw pressed on a rubber bulb at the rear of the pipette to control the flow of fluid. The vessel could be sucked easily into the tip of the pipette with the dissection fluid and then expelled into the cannulation chamber. A flat field objective was needed to provide a wide field for viewing the vessel as it was introduced into the cannulating chamber. It was necessary to ensure that solutions contained protein during all transfer operations and that they were cold, to prevent the vessel from sticking to the wall of the pipette.

Cannulation, Microscope, and Tissue Chamber

The apparatus we used to cannulate isolated microvessels was adapted with minor modifications from a design originally developed by Burg et al[7] for use on isolated kidney tubules.

To perfuse a suitable vessel, a perfusion-holding pipette engaged one end of the vessel by gentle suction, and the perfusion pipette was advanced into the lumen (Fig. 1). The vessel was then aspirated to achieve as tight a seal as possible. A third, fluid-exchange, pipette was inserted into the perfusion pipette. Appropriate valves were adjusted to place the perfusion fluid into the tip of the perfusion pipette within seconds, while draining waste fluid out. In this way, a variety of solutions could be tested on a single vascular segment. The other end of the vessel was then aspirated into another micropipette (a collection-holding pipette), with a tip diameter approximately equal to that of the vessel. The quality of the seal was improved by precoating the pipettes with encapsulating resin (Sylgard 184; Dow Corning, Midland, MI). The tip of the collection-holding pipette was filled with water-equilibrated mineral oil, which prevented evaporation but caused no significant resistance to flow. All accumulated fluid was collected at periodic intervals into a calibrated pipette.

The pipettes were mounted in acrylic holding pieces fitted within specifically designed aluminium V-Tracks (White instruments, Suitland, MD) (Fig. 2).[12] Each V-Track was mounted at a 30° angle to the horizontal plane atop a micromanipulator (Brinkman; White Instruments), which provided movement along both axes of the horizontal plane. The pipette arrangement moved vertically by elevating column supports (J. H. Emerson, Cambridge, MA) that were positioned below the micromanipulator.

The perfusion chamber was mounted above an inverted microscope (Olympus IMT 2; Scientific Supply), similar to the one described by Burg et al.[7] The perfusion chamber held approximately 0.5 ml of bathing medium, which was exchanged continuously throughout the course of an experiment without disturbing the vessel. The temperature of the fluid in the chamber was monitored by a Temperature Controller (Yellow Springs Instrument, Yellow Springs, OH), and the output of the heater was regulated by a

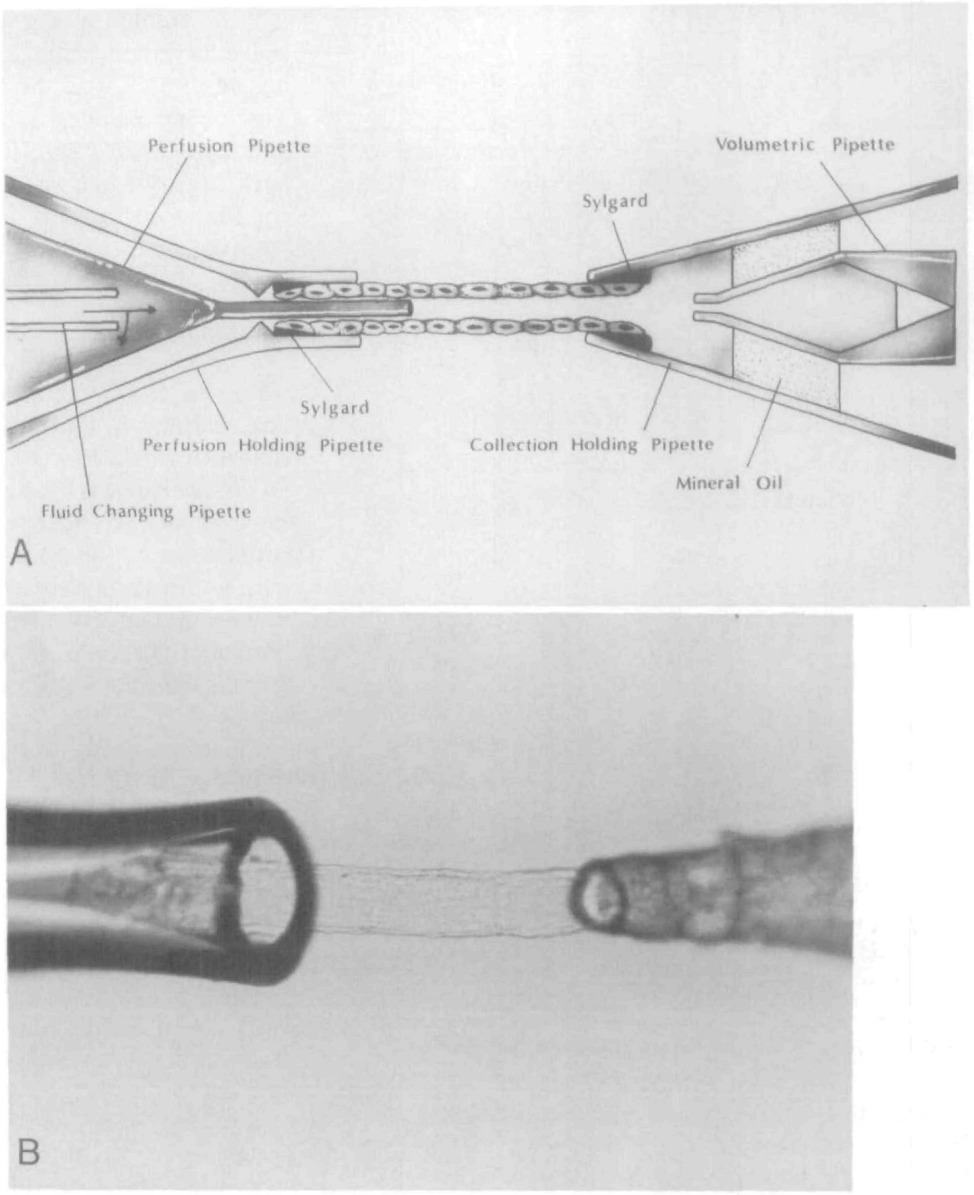

Fig. 1. (A) Schematic of a cannulated retinal vessel. (B) The cannulated retinal vessel is 0.25 mm long and has an outside diameter of 0.06 mm. As in the schematic, the perfusion-holding pipette on the left, and the collection-holding pipette is on the right. (×40)

feedback controller. The bathing medium pH and PO_2 was regulated with a gas mixture (93% O_2, 7% CO_2).

The size and shape of the pipettes were critically important to the success of the experiments. A microforge equipped with a microscope (Stoelting, Chicago, IL) was used to form the tips and shapes of the pipettes. It was necessary for the holding-perfusion and perfusion pipettes to be concentric, and for the perfusion pipette to be pulled down into a long straight tip with an external diameter of 15–22 μm. More complex was the perfusion-holding pipette, which had one constriction with a diameter of 21–28 μm and an outer opening of 85 μm. The collection-holding pipette had an opening slightly smaller than the diameter of the vessel, approximately 35 μm. The volumetric collecting pipette was designed so that the expected perfusion rate and the desired collection time would determine the necessary volume of the pipette.

The physiologic solution used in these experiments was a modified Krebs Ringer bicarbonate buffer (KRBB; 25 mM, 297 mOsm/kg), which was composed of 114 mM NaCl, 1.9 mM K_2HPO_4, 10 mM Na acetate, 0.5 mM $MgSO_4$, 0.7 mM $CaCl_2$, 5.6 mM alanine, 2.5 mM dextrose, and 25.0 mM $NaHCO_3$. The solution was bubbled with 93% O_2/7% CO_2 in the perfusion chamber. Preliminary studies showed that 7% CO_2 maintained the bath at pH 7.4 at 37°C.

Absence of plasma proteins appeared to increase the hydraulic conductivity and permeability of the capillary wall to small solutes and to decrease the

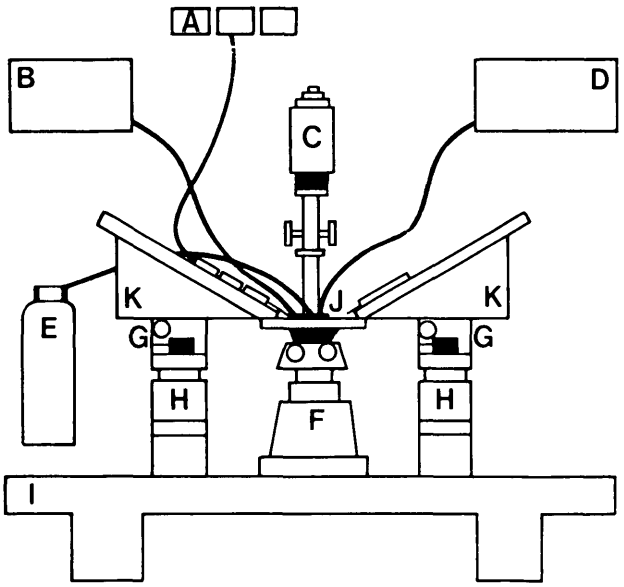

Fig. 2. Schematic of the experimental apparatus. A, perfusate reservoir; B, pump; C, light source; D, temperature controller; E, O_2/CO_2 gas source; F, inverted microscope; G, micromanipulator; H, elevator; I, stable base; J, chamber; K, V-track. Modified from Chonko AM, Irisch JM, III, and Welling DJ: Methods Find Exp Clin Pharm 4(B):221, 1978.[12] See text for detailed description of apparatus.

selectivity of the wall to macromolecules. We had demonstrated this phenomenon by replacing the serum with 1% albumin in three experiments. Accordingly, sterile normal rabbit serum was maintained at 4% in both the perfusate and the bath in order to preserve the endothelial properties and the osmotic equilibrium across the vessel wall.

Once the vessels were mounted on the microperfusion apparatus, they were perfused with 0.3% trypan blue in the physiologic solution, to allow rapid detection of any macroscopic vascular tear created during dissection. Tryptan blue was advantageous in that it rapidly identified microscopic holes and also stained damaged cells.[13]

The vessels could leak at two sites: at points where the endothelial cells have been inadvertently crushed or pinched during the isolation procedure, and at branch points where capillary-sized vessels leave the main vessel (so-called hairpin capillary loops, which dip into the natural spaces between the nerve fibers and are severed when the larger vessel is peeled from the nerve fiber layer during dissection). Leaking vessels were discarded and replaced until one that had no leaks was mounted. Occasionally, if a branch point was close to the collection pipette, it could be drawn inside the collection pipette and the vessel used for perfusion experiments.

In all studies, a 45-min equilibration period preceded the experiment. During this time the vessel was heated to 37°C and the perfusion rate was adjusted. Three control collections were performed at the beginning of each study; then the appropriate bath or perfusion change was performed, followed by an equilibration period of at least 10 min. This procedure was repeated for each experimental episode.

Determination of Radioactivity

For ^{14}C and ^{3}H determinations, aliquots of perfusion, collection, and bathing fluids were placed in vials with 0.5 ml of acetic acid, to which was added 10 ml of Scintiverse II (Fisher Scientific, Fair Lawn, NJ). Samples were counted on a Beckman model LS7000 liquid scintillation counter, the windows of which were adjusted to give <0.1% ^{3}H activity in the ^{14}C channel and 25–30% ^{14}C activity in the ^{3}H channel.

Standard techniques were used to correct count rates to activities for each isotope.

Protocols

These studies followed a series of planned steps to test the preparation for the investigation of transport across retinal vessels.

Dilution of inulin and fluid flux across retinal vessels: A perfusate containing 100 μCi/ml of methoxy-^{3}H inulin (specific activity, 385.5 mCi/g) was passed through isolated retinal vessels, and its dilution (collected vessel inulin fluid counts per perfusate counts of inulin per unit volume; C_L^i/C_o^i) and fluid flux (J_v) were determined.

The fluid flux J_v (absolute volume of fluid transported, in nl/min/mm), was calculated, as described previously[8,9] from the difference between the rates of collection (V_L) and perfusion (V_o), and normalized per millimeter of perfused retinal vessel length (L):

$$J_v = \frac{V_L - V_o}{L} \quad (1)$$

Quantitative comparisons of transport rates usually are based on a flux per unit length. Changes in vessel diameter induced by differing perfusion pressures and the outflow constriction at the collection end have appeared to make calculations based on surface area less accurate.[14] The rates of perfusion (V_o) and collection (V_L) were obtained easily from the experiment. V_o (nl/min) was calculated from the rate of collection of ^{3}H inulin:

$$V_o = \frac{C_L^i \, Vcp}{C_o^i \, t} \quad (2)$$

Where C_L^i Vcp is the total amount of radioactivity in the collecting calibrated pipette, and Vcp is the volume of the calibrated collecting pipette; C_o^i is the concentration of inulin in the perfusion fluid; and t is the duration of the collection period. V_L (nl/min) was determined directly from the time required to fill the calibrated micropipette.

Fluorescein dilution in reference to inulin: Lumen-to-bath fluorescein fluxes were measured from the rates of loss of radioactively labeled fluorescein from the luminal perfusate in reference to inulin.

The perfusate contained 5 μCi/ml of 9-carboxy-^{14}C sodium fluorescein (original specific activity, 18.48 mCi/mmol) together with 100 μCi/ml ^{3}H inulin for perfusion rates and fluid flux measurements.

The fluorescein lumen to bath flux was computed as the difference between perfused and collected amounts of fluorescein, normalized per millimeter vessel length, and calculated as

$$Jl \underset{Fluor}{\rightarrow} b = \frac{V_o C_o^f - V_L C_L^f}{L} \quad (3)$$

where $Jl \underset{Fluor}{\rightarrow} b$ is the lumen-to-bath fluorescein flux ($\times 10^{-12}$ mol/min/mm); C_o^f and C_L^f are the measured concentrations of fluorescein in the perfusate and the collected fluids; V_L is the measured collection flow rate; and V_o is the perfusion rate, calculated from the change in inulin concentration.

Net lumen to bath fluorescein flux measurements were performed in six retinal vessel segments, before and after competitive inhibition by probenecid. In some vessel segments, the probenecid effect was tested first in the perfusate and then in the bath. After three to four initial determinations of the ^{3}H inulin and ^{14}C fluorescein dilutions in each vessel, probenecid (3.25×10^{-4} M) was added either to the perfusate or to the bath.

In four experiments, the viability of the preparation (approximate survival time) was tested by examining the lumen-to-bath fluorescein flux at different time intervals, up to 5–6 hr after vessel dissection.

In another series of four experiments, we studied the behavior of the net outflux of fluorescein with increasing concentrations of probenecid in the bath (3.25×10^{-6} M, 3.25×10^{-5} M, and 3.25×10^{-4} M).

Bath-to-lumen fluorescein fluxes across retinal vessels: Bath-to-lumen fluorescein fluxes $Jb \underset{Fluor}{\rightarrow} l$ were computed from the rate of appearance of ^{14}C-labeled fluorescein in the collected luminal solution, when the initial perfusate contained no fluorescein. ^{14}C fluorescein was added to the bathing solution to a total activity of 3–5 μCi/ml. The perfusate contained 60–100 μCi/ml of ^{3}H inulin to determine the perfusion rate and fluid flux across the retinal vessels.

After three to four determinations in each vessel with only ^{3}H inulin in the perfusate, ^{14}C fluorescein was added to the bath.

The influx (secretion) of fluorescein from bath to lumen was calculated as proposed by Shimomura et al,[15] as

$$Jb \underset{Fluor}{\rightarrow} l = \frac{V_L C_L^f}{L} \quad (4)$$

where $Jb \underset{Fluor}{\rightarrow} l$ is the secretion rate ($\times 10^{-12}$ mol/min/mm); V_L is the rate of vessel fluid collection; C_L^f is the concentration of ^{14}C fluorescein in the collected fluid; and L is vessel length. To examine the movement of fluorescein from bath to lumen under competitive inhibition, probenecid (3.25×10^{-4} M) was added later to the bath.

The fluorescein fluxes were calculated after normalizing fluorescein percent dilution to inulin.

Coupling of fluorescein transport with fluid flux in retinal vessels: The relationship between fluorescein transport and net fluid secretion was studied under a variety of conditions: 1) with increasing concentrations of fluorescein in the bath; 2) with fluorescein in the perfusate; 3) under competitive inhibition (probenecid), either in the perfusate or bath, when fluorescein was either perfused or only added to the bath; and 4) with increasing concentrations of probenecid in the bath when fluorescein was perfused.

Statistical analysis: Measurements for a given vessel were averaged for each experimental period. In general, there were four or five fluorescein flux and J_v measurements in each period. The mean values from individual vessels then were used to compute an overall mean and standard error of the mean. Means from different groups of vessels were compared by the student t-test.

Results

Dilution of Inulin and Fluid Flux Across Retinal Vessels

When ^{3}H inulin was perfused through the retinal vessel segments, its dilution (C_L^i/C_o^i ratios) remained at 80.2 ± 2.3% over a fairly wide range of perfusion rates (5.2–18.5 nl/min; Table 1).

This dilution was due apparently to fluid flux from bath to lumen across the retinal vessels. The total radioactivity due to ^{3}H inulin in each collected sample varied from 4000 to 7000 counts per 10 min. If

10% of the label had been lost into the bath during the 10-min collection period, then the total bath counts would have varied from 400 to 700 counts per 10 min. However, when the total bath was measured, there were no detectable counts. We believe, therefore, that ^{3}H inulin was a suitable volume marker. Tissue uptake of ^{3}H inulin probably was not a source of error, since each vessel was perfused for at least 15 min before the first collection, a period which allowed more than adequate time for equilibration of ^{3}H inulin in a tissue with less than 1 nl total volume.[9]

The fluid flux from bath to lumen across the retinal vessels was calculated as 6.3 ± 1.0 nl/min/mm for perfusion rates of 6.6 ± 0.2 nl/min. Higher perfusion rates (15.2 ± 0.3 nl/min) caused an increase in water reabsorption (20.3 ± 2.8 nl/min/mm) and an increase in tracer dilution. To test the effect of the perfusion rate on the experimental preparation and dilution values of the reference tracer, we examined, in the same vessel, the correlation between fluid flux and perfusion rate. When perfusion rates were maintained at values of less than 10 nl/min, dilutions were reproducible and independent of the perfusion rates. However, when the perfusion rates reached values higher than 10 nl/min, more variability was apparent.

A lower albumin concentration in the perfusate increased markedly the permeability of the retinal vessels, as shown by higher inulin dilutions. When the concentration of albumin was decreased from 4% to 1% in the physiologic solution both in the perfusate and bath, the C_L^i/C_o^i ratios were only 55.1 ± 5.2% (three experiments), with perfusion rates of 7.1 ± 1.3 nl/min.

Fluorescein Dilution in Reference to Inulin

When ^{14}C fluorescein was perfused simultaneously with the reference tracer, its dilution (C_L^f/C_o^f ratio) remained at 81.9 ± 3.8% over a wide range of perfusion rates (Table 1). The values for fluorescein dilution were strikingly similar to those obtained for inulin.

In order to examine the survival time and functional viability of the preparation, we saw that lumen-to-bath fluorescein fluxes remained fairly constant for the first 4 hr; thereafter, increases of 30–83% occurred (Fig. 3). All experiments therefore were performed within a 4-hr time interval.

Net lumen-to-bath fluorescein measurements before and after competitive inhibition by probenecid are shown in Figure 4. The initial perfusate contained 2.5×10^{-4} M of ^{14}C fluorescein, with perfusion rates varying from 3.9 to 6.3 nl/min. The extremely low lumen to bath fluorescein flux values, 0.5 ± 0.9 $\times 10^{-12}$ mol/min/mm, increased by 68% ($0.05 < P \leq 0.1$) when probenecid was added to the perfusate and by 210% ($0.01 < P \leq 0.025$) when probenecid was placed in the bath.

As higher concentrations of probenecid were added to the bath, we found that the lumen-to-bath fluorescein flux values also increased (Fig. 5; comparing with baseline, $0.01 < P \leq 0.025$, $0.0005 < P \leq 0.005$, and $0.0005 < P \leq 0.005$, for probenecid concentrations of 3.25×10^{-6} M, 3.25×10^{-5} M, and 3.25×10^{-4} M, respectively). The flattening of the curve at the higher probenecid concentrations in the bath appeared consistent with a saturable process of fluorescein reabsorption.

Since the bath volume was approximately 0.5 ml and the total fluid perfused during the course of an experiment was approximately 1 μl, fluorescein concentrations in the bath solution were insignificant in comparison to those in the luminal solution, under all experimental conditions. Accordingly, any error due to backflux of fluorescein from bathing solution to the lumen could be neglected.

Table 1. Results obtained with the reference tracer ^{3}H-inulin and ^{14}C-fluorescein in seven experiments

Vessel length (L) (mm)	*C_L/C_0 (%) inulin*	*Time (min)*	*Pipette size (nl)*	*V_L (nl/min)*	*V_0 (nl/min)*	*$V_L - V_0$ (nl/min)*	*J_v (fluid flux), (nl/min/mm)*	*C_L/C_0 fluorescein*
0.25	80.5 ± 2.2	6.5 ± 1.3	47.7	7.8 ± 1.6	6.3 ± 1.5	1.5 ± 0.1	5.9 ± 0.5	72.3 ± 1.8
0.32	71.9 ± 0.7	6.6 ± 0.8	47.4	7.5 ± 0.8	5.4 ± 0.6	2.1 ± 0.3	6.6 ± 0.7	84.6 ± 1.1
0.28	81.5 ± 1.4	7.3 ± 0.4	47.0	6.4 ± 0.3	5.2 ± 0.3	1.2 ± 0.1	6.4 ± 0.6	80.6 ± 1.4
0.25	84.2 ± 0.3	5.2 ± 0.8	47.0	9.6 ± 1.4	8.0 ± 1.2	1.6 ± 0.2	6.1 ± 0.9	89.6 ± 0.7
0.18	89.3 ± 1.6	5.6 ± 0.7	110.3	20.5 ± 2.4	18.5 ± 2.4	2.0 ± 0.1	11.2 ± 0.5	86.7 ± 1.6
0.22	80.0 ± 0.6	5.7 ± 0.2	108.0	19.1 ± 0.7	15.2 ± 0.6	3.9 ± 0.1	17.4 ± 0.5	65.8 ± 1.2
0.37	73.7 ± 0.9	5.5 ± 0.1	110.1	20.3 ± 0.4	15.0 ± 0.4	5.3 ± 0.1	14.5 ± 0.4	94.1 ± 0.3
Total	80.2 ± 2.3							81.9 ± 3.8

Each value represents mean ± SE of three to seven collection periods. Shown are the percent dilution of collected fluid (C_L/C_0), the collection rate (V_L), perfusion rate (V_0), net fluid entry ($V_L - V_0$), vessel length (L), and fluid flux (J_v) for each experiment.

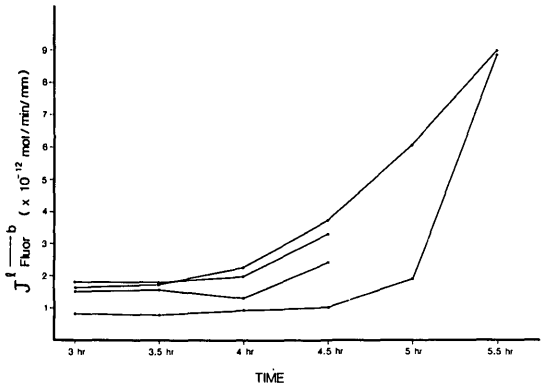

Fig. 3. Relationship between flux of fluorescein from lumen to bath (J^{l}_{Fluor} → b) and duration of the experiment.

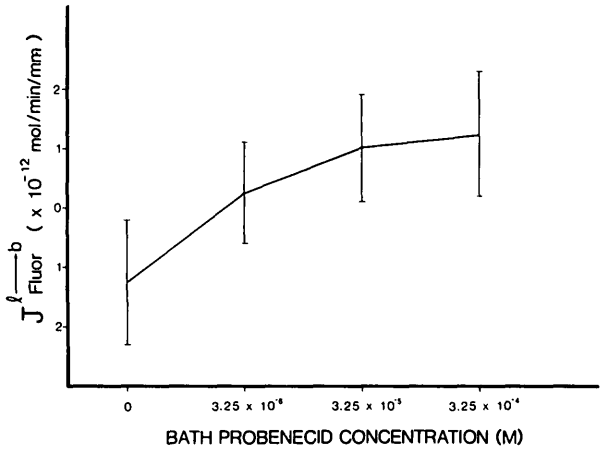

Fig. 5. Lumen-to-bath flux of fluorescein (J^{l}_{Fluor} → b) is plotted as a function of bath probenecid concentration (four experiments). Means and SEs (vertical line segments) are given.

Bath-to-Lumen Fluorescein Fluxes Across Retinal Vessels

When ^{14}C fluorescein was added to the bath, with only ^{3}H inulin in the perfusate, fluorescein rapidly moved from bath to lumen across the retinal vessel walls, reaching a concentration in the collection fluid 1.3 times the concentration of the initial fluorescein bath, resulting in perfusion rates of 6.4–7.5 nl/min and time periods not exceeding 10 min. When the perfusion rates were slowed to 0.3 nl/min, the fluorescein concentration in the collection fluid became as high as 40 times that in the bath.

The values of J^{b}_{Fluor} → l for higher perfusion rates (6.4–7.5 nl/min) and with different concentrations of fluorescein in the bath are presented in Figure 6. Even with fluorescein concentrations in the bath lower than those in the lumen, the bath-to-lumen fluorescein fluxes were always much higher than the lumen-to-bath fluorescein fluxes. All retinal vessel segments showed a concentration-dependent flux of fluorescein from bath to lumen that increased with increasing fluorescein concentrations in the bath. Again, the flattening of the curve at higher fluorescein levels in the bath appears consistent with the Michaelis-Menten equation. The average Michaelis constant (Km) was 1.1×10^{-4} M. When probenecid was added to the bath, much less fluorescein moved from bath to lumen (Fig. 6; $0.025 < P \leq 0.05$, $0.01 < P \leq 0.025$, and $0.01 < P \leq 0.025$, for fluorescein concentrations of 0.87×10^{-4} M, 1.5×10^{-4} M, and 2.5×10^{-4} M, respectively.

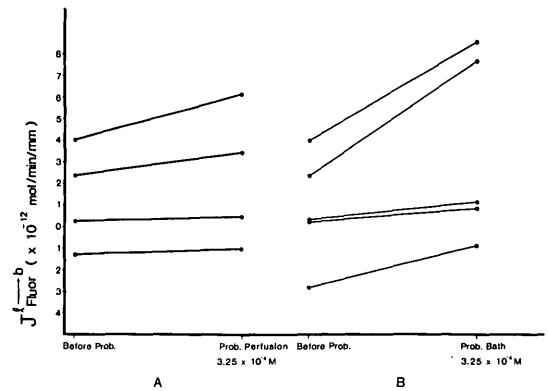

Fig. 4. Effect of probenecid (Prob.) on the flux of fluorescein from lumen to bath (J^{l}_{Fluor} → b). (A) Probenecid in the perfusate; (B) probenecid in the bath.

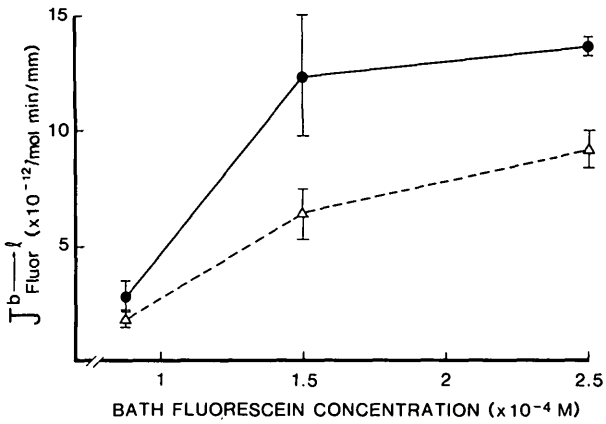

Fig. 6. Relationship between the fluorescein concentrations in the bath and the flux of fluorescein from bath to lumen (J^{b}_{Fluor} → l) before (solid line) and after (dashed line) addition of probenecid (3.25×10^{-4} M) to the bath (10 experiments). Means (circles, before probenecid; triangles, after probenecid) and SEs (vertical line segments) are given.

In all experiments, no correlation of $Jb \xrightarrow[\text{Fluor}]{} l$ with elapsed time was observed, indicating that the system was in a steady state.

Coupling of Fluorescein Transport with Fluid Flux in Retinal Vessels

Net fluid secretion across the retinal vessels in response to increasing concentrations of fluorescein in the bath is illustrated in Figure 7. In the initial control period, net fluid flux was 6.3 ± 1.0 nl/min/mm with perfusion rates of 6.6 ± 0.2 nl/min. After the addition of 1.5×10^{-4} M fluorescein to the bath, the rate of net fluid secretion increased by 36% ($0.0005 < P \leq 0.005$), and increased by 60% ($P \leq 0.0005$) when a concentration of 2.5×10^{-4} M of fluorescein was added to the bath. In another set of experiments, when fluorescein was added to the perfusate (2.5×10^{-4} M), there was a smaller increase in the rate of net fluid secretion (a mean of 17% from a total of 16 experiments; data not shown).

To examine further the coupling of fluorescein transport with fluid secretion, we studied the effect of probenecid on the rate of fluid secretion. First, fluorescein added to the bath always caused an increase in net fluid flux across the retinal vessel walls. The subsequent addition of probenecid (3.25×10^{-4} M) inhibited fluid flux by approximately 39% ($0.01 < P \leq 0.025$) for a concentration of 1.5×10^{-4} M and by 28% ($0.01 < P \leq 0.025$) for a concentration of 2.5×10^{-4} M of fluorescein in the bath (Fig. 7).

A similar situation occurred when fluorescein was present in the perfusate. Subsequent additions of probenecid to the perfusate decreased net fluid flux

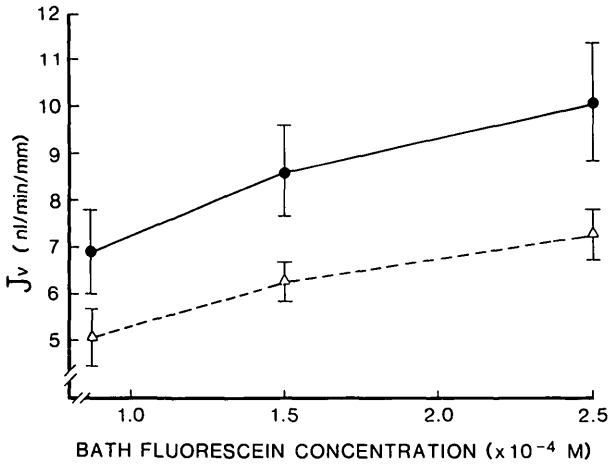

Fig. 7. Relationship between the fluorescein concentration in the bath and the fluid flux (J_v) before (solid line) and after (dashed line) addition of probenecid (3.25×10^{-4} M) to the bath (10 experiments). Means (circles, before probenecid; triangles, after probenecid) and SEs (vertical line segments) are given.

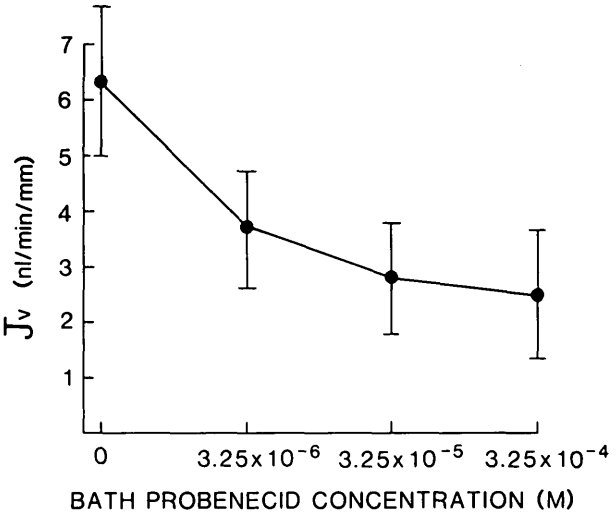

Fig. 8. Fluid flux (J_v) is plotted as a function of bath probenecid concentrations (four experiments). Means and SEs (vertical line segments) are given.

by approximately 22%, and by approximately 61% when added to the bath. When increasing concentrations of probenecid were added to the bath (3.25×10^{-6} M, 3.25×10^{-5} M, and 3.25×10^{-4} M), a dose-dependent effect was observed again: the fluid flux decreased with increasing concentrations of probenecid in the bath (Fig. 8).

Finally, we verified that the fluid flux measured in the isolated retinal vessel preparations is temperature-dependent. When the temperature was decreased to 13°C in four experiments, the rate of fluid secretion was reduced by 19–35%. This effect was reversed easily when the temperature was increased, and fluid flux values were restored to previous levels (data not shown).

Discussion

Our findings show that microperfusion studies of the rabbit retinal vessels are feasible, reproducible, and may yield important data to our understanding of retinal vascular physiology. Specifically, we found 1) a unidirectional movement of fluorescein across the retinal vessel walls, which may be due to a more general active transport for organic anions; 2) evidence for a net fluid flux from outside the vessel walls to the lumen; and 3) stimulation of this fluid flux by the fluorescein transport.

Throughout the study we used the conventional method of measuring net fluid transport in isolated renal tubules.[8,9] In the kidney, fluid movements were calculated in tubules perfused with a volume marker such as inulin or albumin; the perfusate was collected quantitatively from the distal end of the tubule in a pipette; and from the change in the concentration of

the volume marker, the amount of fluid absorbed by the tubule was determined.[8,9]

The perfused vascular segments studied were relatively short, in order to avoid branchings and consequent leaks. This shortness initially was a source of concern, but we found that reproducible changes could be detected even with these relatively short retinal vascular segments.

When fluorescein was added to the perfusate, its dilution remained at the same level as that of inulin, suggesting minimal or no movement of fluorescein from lumen to bath. This observation was noteworthy because of the difference in molecular size between fluorescein and inulin. If the retinal vessel wall behaved as a semipermeable barrier to fluorescein, movement from lumen to bath would be larger than with inulin.

When fluorescein was added to the bath, its passage across the retinal vessel walls rapidly resulted in concentrations in the lumen that reached levels as high as 40 times those in the bath. This concentrating effect was better achieved when lower perfusion rates were used. Using faster perfusion rates, this movement of fluorescein from bath to lumen was clearly concentration-dependent, and it increased with higher concentrations of fluorescein in the bath. The flattening of the curve at higher bath fluorescein levels appears consistent with a saturable process. Furthermore, the upper limit of the rate of transport was obtained with fluorescein concentrations similar to those presented by Cunha-Vaz and Maurice.[4]

The observation that fluorescein when placed only in the bath could be brought to higher concentrations in the lumen demonstrates movement against an uphill gradient. This striking difference in the movement of fluorescein from bath to lumen and lumen to bath in the same experimental conditions supports the existence of a unidirectional movement of fluorescein across the retinal vessel walls.

When probenecid, a competitive organic anion transport inhibitors, was added to the bath, it increased markedly the fluorescein movement from lumen to bath, and inhibited fluorescein uptake into the lumen.

The observed saturation kinetics of the fluorescein movement across the retinal vessel walls; the specific inhibition of fluorescein movement by a competitive inhibitor; its unidirectional characteristics; and its maintenance in a situation of uphill gradient all support the idea that an active transport process was involved.

Active transport of organic anions such as iodopyracet[16] and fluorescein[4] have been postulated to occur from vitreous to blood across the retina and retinal vessels. More recently, a similar active outward transport of fluorescein was reported in the anterior uvea[17] and choroid plexus[18] of the rabbit, with Km values of 1.2×10^{-4} M and 4×10^{-5} M, respectively. The Km for fluorescein observed in our study, 1.1×10^{-4} M, is in the same range. Our findings are the first direct demonstration of an active outward movement of fluorescein across the retinal vessel walls.

The observation that competitive inhibition by probenecid is significantly more effective when it is in the bath suggests a difference between the basal and luminal membranes of the retinal vascular cells involved in the organic anion transport, presumably the endothelial cells.

An important finding was the observation of a surprisingly high fluid flux across the retinal vessel wall from bath to lumen. This bath-to-lumen fluid flux remained constant when perfusion rates of less than 10 nl/min were used. However, variable values of fluid flux were observed with perfusion rates higher than 10 nl/min. As perfusion rates increased, C_L^i/C_o^i ratios decreased, but fluid flux increased, and small errors became magnified. We felt that high rates of perfusion yielded less reliable results. Therefore, throughout our studies, we used perfusion rates of less than 10 nl/min.

This bath-to-lumen fluid flux was temperature-dependent and appeared to be coupled to the organic anion transport. Fluorescein stimulated the fluid flux by 17% when added to the perfusate and by 60% when added to the bath. It was also partially inhibited by probenecid. A fluid flux coupled to the active transport of an organic anion, p-aminohippuric acid, has been shown to occur in the proximal straight tubule. The involvement of the sodium–potassium pump, as shown by its inhibition by ouabain, was one of explanations offered.[19]

Although there is indirect evidence for interstitial fluid secretion in the brain,[20] similar studies in isolated preparations of brain vessels are lacking, namely because of problems associated with the mechanical or enzymatic homogenization procedures used for isolation.[21]

The retinal vessels may function as selective tubules which facilitate the penetration of oxygen and glucose into the retina, but may have a very active fluid flux from the retina into the blood, which keeps the retina relatively dry and maintains the appropriate environment for optimal neural tissue function.

Any alteration of these transport systems may be of major clinical significance. Macular edema is an important cause of visual loss and is frequently concomitant in retinal vascular disease. Recently, when reviewing basic concepts of retinal edema,[22] we dis-

cussed the importance of a variety of factors in its development, such as plasma and tissue osmotic pressure, blood–retinal barrier diffusion, capillary and tissue hydrostatic pressure, and tissue compliance. Alterations of fluid flux from retina and vitreous to blood may well be the principal cause of retinal edema. Further studies are needed to characterize this fluid flux across the retinal vessel walls and its dependence on other ionic movements.

The development of this new experimental model for microperfusion studies of the rabbit retinal vessels has opened new perspectives for future research in retinal vascular physiology and pharmacology.

Key words: retinal vessels, fluorescein, microperfusion, permeability, fluid flux

Acknowledgments

Dorris Brown prepared the manuscript, and Maxine Gere edited it.

References

1. Cunha-Vaz JG, Faria de Abreu, Jr, Campos AJ, and Figo GM: Early breakdown of the blood–retinal barrier in diabetes. Br J Ophthalmol 59:649, 1975.
2. Goldberg MF: Diseases affecting the inner blood–retinal barrier. *In* The Blood–Retinal Barriers, Cunha-Vaz JG, editor. New York, Plenum Press, 1979, p. 309.
3. Cunha-Vaz JG: The blood–ocular barriers. Surv Ophthalmol 23:279, 1979.
4. Cunha-Vaz JG and Maurice DM: The active transport of fluorescein by retinal vessels and the retina. J Physiol (Lond) 191:467, 1967.
5. Palestine AG and Brubaker RF: Pharmacokinetics of fluorescein in the vitreous. Invest Ophthalmol Vis Sci 21:542, 1981.
6. Tsuboi S, Fujimoto T, Uchihori Y, Emi K, Lizuka S, Kishida K, and Manabe R: Measurement of retinal permeability to sodium fluorescein in vitro. Invest Ophthalmol Vis Sci 25:1146, 1984.
7. Burg MB, Grantham J, Abramow M, and Orloff J: Preparation and study of fragments of single rabbit nephrons. Am J Physiol 210:1293, 1966.
8. Burg MB and Orloff J: Control of fluid absorption in the renal proximal tubule. J Clin Invest 47:2016, 1968.
9. Kokko JP: Sodium chloride and water transport in the descending limb of Henle. J Clin Invest 49:1838, 1970.
10. Cunha-Vaz JG, Shakib M, and Ashton N: Studies on the permeability of the blood–retinal barrier: I. On the existence, development and site of a blood–retinal barrier. Br J Ophthalmol 50:441, 1966.
11. Shakib M and Cunha-Vaz JG: Studies on the permeability of the blood–retinal barrier: IV. Junctional complexes of the retinal vessels and their role in the permeability of blood–retinal barrier. Exp Eye Res 5:229, 1966.
12. Chonko AM, Irisch JM, III, and Welling DJ: Microperfusion of isolated tubules. Methods Find Exp Clin Pharm 4(B):221, 1978.
13. Kokko JP: Transport characteristics of the thin limbs of Henle. Kidney Int 22:449, 1982.
14. Jacobson HR: Transport characteristics of in vitro perfused proximal circonvoluted tubules. Kidney Int 22:425, 1982.
15. Shimomura A, Chonko AM, and Grantham JJ: Basis for heterogeneity of para-aminohippurate secretion in rabbit proximal tubules. Am J Physiol 240:430, 1981.
16. Becker B and Forbes M: Iodopyracet (diodrast) transport by the rabbit eye. Am J Physiol 240:461, 1961.
17. Stone RA and Wilson CM: Fluorescein transport in the anterior uvea. Invest Ophthalmol Vis Sci 22:303, 1982.
18. Bresler SE, Bresler VM, Kazebekov EN, Nikiforov AA, and Vasilieva NN: On the active transport of organic anions (fluorescein) in the choroid plexus of the rabbit. Biochim Biophys Acta 550:110, 1979.
19. Grantham JJ: Studies of organic anion and cation transport in isolated segments of proximal tubules. Kidney Int 22:519, 1982.
20. Bradbury M: The Concept of a Blood–Brain Barrier. Bath, Pitman Press, 1979, p. 254.
21. Pardridge WM: Brain metabolism: A perspective from the blood–brain barrier. Physiol Rev 63:1481, 1983.
22. Cunha-Vaz JG and Travassos A: Breakdown of the blood–retinal barriers and cystoid macular edema. Surv Ophthalmol 28:485, 1984.